THE JOURNAL OF PHYSICAL CHEMISTRY B

ARTICLE

pubs.acs.org/JPCB

Understanding the Equilibrium Ion Exchange Properties in Faujasite Zeolite from Monte Carlo Simulations

Marie Jeffroy,[†,‡] Anne Boutin,[‡] and Alain H. Fuchs[*,§]

[†]IFP Energies Nouvelles (IFPEN), 1 et 4 avenue de Bois-Preau, 92852 Rueil-Malmaison, France

[‡]Ecole Normale Superieure, Departement de Chimie, CNRS-ENS-UPMC, 24 rue Lhomond, 75005 Paris, France

[§]CNRS, Paris, France

ABSTRACT: We have adapted a grand ensemble Monte Carlo simulation method to directly compute, for the first time to our knowledge, univalent cation exchange isotherms in zeolites. The computed isotherms for the exchange of sodium in NaY faujasite by lithium, potassium, rubidium, and cesium ions, respectively, are in good agreement with the experimental ones. They display the three main types of behavior observed in zeolites, namely, a monotonous evolution of selectivity throughout the exchange process (Li^+), a selectivity reversal (K^+), and an incomplete exchange (Rb^+ and Cs^+). The initial stage of the cation exchange is shown to be dominated by the hydration energy of the cations in the external aqueous solution. The final part of the process is often dominated by the cation−framework and cation−cation interactions. A crossover between these two regimes explains the frequently observed reversal of selectivity phenomenon. The incomplete exchange observed in the case of Rb^+ and Cs^+ is shown to correspond to a blocked state of the system for highest accessible composition of the aqueous solution. This stable state is shown not to be linked to an inability of the cesium cations to cross the six-ring window in order to penetrate into the smallest cages.

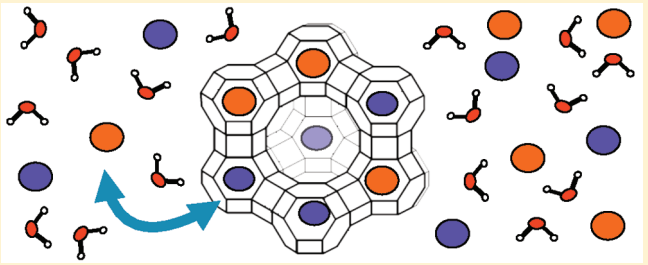

INTRODUCTION

Extraframework cation exchange is a very important property of zeolites.[1] It has been used in a wide variety of applications, from water softening in detergency[2] to selective removal of radionuclides (such as cesium) from liquid nuclear waste.[3] It is currently being used in the decontamination process of highly radioactive water resulting from the accident at Fukushima Daiichi nuclear power plant.[4] Cation exchange is known to deeply modify the adsorption behavior and selectivity of a given zeolite, as well as its catalytic activity. This has led to extensive experimental studies of cation location for almost all known zeolite types, with many different cations, such as alkaline, alkaline earth, or transition metal cations, using X-ray diffraction (XRD), NMR, and other spectroscopic techniques.[5,6] A large number of computer simulation methods and theoretical models have also been developed for this purpose.[7−12] Recently an extensive review of the extraframework cation distributions in X and Y faujasites has been proposed.[13]

The overwhelming quantity of data available on the static extraframework cation distributions has been of great use to zeolite chemists to develop new concepts and processes in the field of selective adsorption and catalysis. On the other hand, the actual physicochemical ion exchange process has attracted much less attention. Several in situ XRD and NMR studies addressed the issue of cation migration upon dehydration, and a link with the exchange process was made,[15,16] but no systematic study has allowed yet one to fully understand the basic principles of the cation exchange mechanism in zeolites at the atomistic level.

At the macroscopic level, the thermodynamics and kinetics of the ion exchange process are well described in the literature.[1,14] It has been stressed that cation selectivities in zeolites do not follow the typical rules that are evidenced by other inorganic and organic exchangers.[14] A full understanding of this observation is still lacking.

The ion exchange equilibrium between two univalent cations A^+ and B^+ (the simplest case which we will consider in this work) is described by the following relation:

$$A_{zeo}{}^+ + B_{sol}{}^+ \leftrightarrow A_{sol}{}^+ + B_{zeo}{}^+ \quad (1)$$

where the subscripts "zeo" and "sol" refer to the ions being either inside the zeolite or in the solution (usually an aqueous solution).

The cation mole fractions ($i = A^+$ or B^+) are defined in the usual way

$$x^i_{zeo} = \frac{n^i_{zeo}}{n^{total}_{zeo}}; \quad x^i_{sol} = \frac{n^i_{sol}}{n^{total}_{sol}} \quad (2)$$

The cation exchange isotherm corresponding to eq 1 is the plot of x^B_{zeo} as a function of x^B_{sol}. In Figure 1 (upper panel) are sketched four experimental exchange isotherms corresponding to the exchange of Na^+ cations (in NaY zeolite) by Li^+, K^+, Rb^+, and Cs^+, respectively.

The separation factor, analogous to a selectivity factor, expresses the preference of the zeolite for one of the cations, A^+ or B^+.

Received: September 20, 2011
Revised: October 29, 2011
Published: November 03, 2011

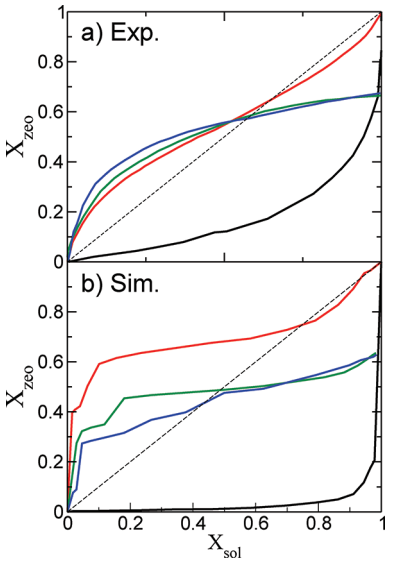

Figure 1. Cation exchange isotherms of NaY zeolite with Li^+ (black line), K^+ (red), Rb^+ (green), and Cs^+ (blue), respectively, at 0.1 total molarity and 298 K. x_{sol} is the mole fraction of the ingoing cation in the aqueous solution. Upper panel: experiments.[17] Lower panel: simulation results (this work).

It is defined as

$$\alpha_A^B = \frac{x_{zeo}^B x_{sol}^A}{x_{sol}^B x_{zeo}^A} \quad (3)$$

$\alpha_A^B = 1$ corresponds to the diagonal in the exchange isotherm plot. If the *ingoing* ion (ion B^+ in eq 1) is preferred, $\alpha_A^B > 1$ and the isotherm lies above the diagonal; $\alpha_A^B < 1$ corresponds to the zeolite being selective for the *outgoing* cation. As an example, the first plot (black line) in Figure 1 (Results and Discussion section) indicates that Na^+ is preferred over Li^+ in the whole range of lithium mole fraction in the aqueous solution.

Apart from α_A^B being always greater (or lower) than 1, two other very interesting types of isotherms were encountered in a certain number of exchange experiments in zeolites. In the first case the selectivity varies with the degree of exchange, and this results in a sigmoidal isotherm, as illustrated by the K^+ isotherm in Figure 1 (red line). In the second case, a complete exchange by the ingoing cation is not reached. This is illustrated by the Rb^+ and the Cs^+ isotherms in Figure 1.

These different types of experimental exchange isotherms have been discussed and interpreted in terms of cation binding with the zeolite framework for different cation sites. "Ion sieving" was also invoked by several authors in order to explain the incomplete exchange isotherms.[1,3,13,14] This means that the ingoing cation would not be able to reach some cationic sites because it is too large to diffuse through the apertures of small cages, for instance. This has been debated in the literature and no firm conclusions have been reached yet.

In this work we report Monte Carlo simulations of the aqueous solution cation exchange of sodium in NaY zeolite, by lithium, potassium, rubidium, and cesium, respectively. These zeolite/cations systems were chosen because they exhibit the three main types of exchange isotherms (see Figure 1), namely, a monotonous evolution of selectivity throughout the exchange process (Li^+), a selectivity reversal (K^+), and an incomplete exchange (Rb^+ and Cs^+).[17] This is the first time, to our knowledge, that equilibrium cation exchange isotherms are directly computed using molecular simulations.

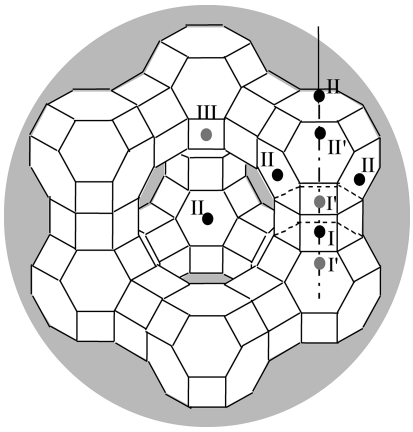

Figure 2. Schematic view of a faujasite supercage with the sites I, I′, II, and III locations.

As described below, the overall agreement between simulated isotherms and experiments is good and allows one to use the simulation results in order to shed some new light onto the exchange process. A careful examination of the relative cation binding energies and a revisit of the exchange thermodynamics in aqueous solutions leads to a comprehensive explanation of the three different types of isotherms encountered in the studied systems.

SIMULATION MODEL AND METHODS

The framework structure of faujasite was taken from the experimental neutron diffraction studies of Fitch et al.[18] The crystalline structure is described in the *Fd*3*m* space group, and the cubic lattice parameter is 24.8536 Å. The framework structure was considered as rigid. One unit cell of faujasite was used as the simulation box, with periodic boundary conditions in all three directions. The cations can occupy different crystallographic sites: sites I are located in the hexagonal prisms which connect the so-called sodalite cages, site I′ are inside the sodalite cages facing sites I, sites II are in front of the six-rings inside the supercages, sites II′ are inside the sodalite cages facing sites II (see Figure 2). Site I has a multiplicity of 16 per unit cell, sites I′, II, and II′ have a multiplicity of 32.

Monte Carlo simulations have been performed in a model $Na_{52}Y$ faujasite (Si:Al = 2.69; 52 cations per unit cell, a unit cell being made of eight supercages). This system was widely used in previous simulation studies of water and hydrocarbon adsorption.[19−21] The cation content is similar to the NaY sample studied experimentally by Sherry[17] (Si:Al of 2.84; 50 cations). In the NaY model an average tetrahedrally bonded (T) atom was used, for reasons detailed in an earlier paper.[20] Average T atom simulations were shown to yield a reasonable description of sodium cation distributions in both dehydrated and hydrated faujasite.[12,21]

Molecular simulations were performed in the classical limit (no bond breaking takes place, for instance). This is justified by the fact that the experimental exchange isotherms are reversible. No hydrolysis is observed experimentally upon univalent cation exchange.[17] The force field used here is solely based on previously published parameters for bulk water (TIP4P model)[22] and cation−framework interactions,[23−25] in a manner described earlier,[21] and with no parameter readjustment. Partial charges on the framework oxygen and T atoms were adjusted in the way

Table 1. Force Field Parameters Used in This Work[a]

	Lennard-Jones: $-4\varepsilon[\sigma^6/r^6 - \sigma^{12}/r^{12}]$		
	σ (Å)	ε (K)	q (|e|)
Li	2.354	38.68	+1
Na	2.586	50.27	+1
K	2.82	62.00	+1
Rb	3.031	58.22	+1
Cs	3.165	59.72	+1
H_2O (TIP4P)	3.154	78.03	$q_H = 0.52$; $q_O = -1.04$
Cl	4.45	50.28	−1
$O_{zeolite}$	3.00	93.53	−0.824 445 1
$Si_{zeolite}$ or $Al_{zeolite}$	–	–	+1.378 071

	Buckingham: $\alpha \exp(-\beta r) - \gamma/r^6$		
	α (K)	β (Å^{-1})	γ (K Å^6)
Li···$O_{zeolite}$	6.11×10^7	4.54	3.305×10^5
Na···$O_{zeolite}$	6.11×10^7	4.05	7.652×10^5
K···$O_{zeolite}$	6.11×10^7	3.53	1.800×10^5
Rb···$O_{zeolite}$	6.11×10^7	3.35	2.300×10^5
Cs···$O_{zeolite}$	6.11×10^7	3.20	2.831×10^5

[a] The Lorentz−Berthelot combination rules [$\sigma_{ij} = (\sigma_{ii} + \sigma_{jj})/2$ and $\varepsilon_{ij} = \sqrt{\varepsilon_{ii}\varepsilon_{jj}}$] are used excepted for the cation−zeolite interaction, where a Buckingham form was used.

described previously,[11] using the electronic structure calculations of Mortier and co-workers.[26] All cations carry a charge of +1 au. Ewald sums were used to calculate the Coulombic terms. All the potential parameters are given in Table 1.

In order to mimic the experimental exchange process, Monte Carlo (MC) simulations must allow a change in the number of cations in the zeolite as well as the number of water molecules. The zeolite system is in contact with a (fictitious) reservoir that represents the aqueous solutions of 0.1 total molarity in order to be able to compare the simulation results to experimental data.[17] Simulations should thus be performed in a semigrand ensemble with the following variables being fixed: $\mu_A, \mu_B, \mu_{water}, N_{cations}, V, T$, where $N_{cations} = (N_A + N_B)$, and μ_A, μ_B, and μ_{water} are the chemical potentials of cations A^+, B^+, and water, respectively.

In addition to the conventional MC moves,[27] we have implemented a new step that allows the mole fractions of the two cations to change within the zeolite, given the external chemical potential constraints and keeping the total number of cations fixed. This is called a "swap" move, in which a cation of type i is replaced by a cation of type j. It corresponds to a combination of the deletion move of the i cation and the insertion move of the j cation at exactly the same location within the zeolite. The probability of accepting such a move is[28]

$$P_{acc}(C_{N_i,N_j} \rightarrow C_{N_i-1,N_j+1}) = \min\left(1, \frac{N_i}{N_j+1}\left(\frac{m_j}{m_i}\right)^{3/2} \exp[\beta(\mu_j - \mu_i)] \exp[-\beta(U_{C_{N_i-1,N_j+1}} - U_{C_{N_i,N_j}})]\right) \quad (4)$$

where m_i and m_j are the masses of cations i and j respectively, $\beta = 1/kT$, and C_{N_i,N_j} denotes a given configuration within the zeolite with N_i cations of type i and N_j of type j.

We note in passing that this swap move is strictly valid for an isovalent cation exchange. If this is not the case (for instance, an exchange of Na^+ by a divalent cation such as Ca^{2+}), the MC step would be slightly more complicated, since the cation exchange must be electroneutral.

As evidenced by eq 4, calculation of the acceptance probability of this swap move requires the sole knowledge of the difference in chemical potential between the A^+ and B^+ cation species in the solution, $(\mu_A - \mu_B)$. Frenkel and co-workers have suggested a way to compute the chemical potential difference between two species in a given solution.[29,30] This method is based on the extension of the test particle method of Widom.[31] We have implemented this method but failed to obtain reliable results. The convergence of the algorithm is extremely slow for a 0.1 M solution (roughly 2 cations per 1000 water molecules).

We have used instead an alternate and indirect method for computing $(\mu_A - \mu_B)$. Taking advantage of the simple relation that holds between the chemical potential of a species i and its mole fraction in the solution

$$\mu_i = \mu_i^0 + RT \ln(\gamma_i x_i) \quad (5)$$

where γ_i is the activity of species i. It comes straightforwardly that

$$\mu_B - \mu_A = \mu_B^0 - \mu_A^0 + RT \ln\left(\frac{\gamma_B}{\gamma_A}\right) + RT \ln\left(\frac{x_B}{x_A}\right) = \Delta\mu^0 + \Delta\mu_{excess} + RT \ln\left(\frac{x_B}{x_A}\right) \quad (6)$$

Now the method used consists of imposing a difference in chemical potential $(\mu_A - \mu_B)$ in the aqueous solution and in directly computing the mole fractions of A^+ and B^+ for different values of the chemical potential difference, through a Monte Carlo simulation. In this simulation, the counterion was the chlorine ion, for which we used the force field proposed by Dang.[25] The results are shown in Figure 3. The simulation results fit nicely with eq 6, considering that the term $\Delta\mu^0 + \Delta\mu_{excess}$ is constant for a given cation, something that is physically reasonable. These fits can thus be conveniently used for computing $(\mu_A - \mu_B)$ for any given cationic mole fraction.

Finally, it should be mentioned that, although the water content within the zeolite does in principle fluctuate, we observed that the actual amount of water was pretty much constant throughout the simulations and that no difference could be found between a simulation with fixed μ_{water} or fixed N_{water}. We thus decided to fix the amount of water to an average equilibrium value of 230 water molecules per unit cell, in order to speed up the MC simulations. We also used the pressure version of parallel tempering for the same purpose of speeding up the relatively complex MC runs.[12,32]

RESULTS AND DISCUSSION

The MC method introduced above enabled us to directly compute the cation exchange isotherms of NaY with Li^+, K^+, Rb^+, and Cs^+. For each sodium mole fraction in the solution, ($x_{Na} = x_A$) and $x_B = (1 - x_A)$, with B = Li^+, K^+, Rb^+, or Cs^+, the chemical potential difference $(\mu_A - \mu_B)$ was computed using eq 6. This value was introduced in eq 4 to compute the probability of acceptance of the cation swap move. A Monte Carlo run was then performed, using this swap move together with the conventional translational and rotational moves and the bias "jump move"[21] consisting of a large displacement by combining deletion and insertion moves. Each run length was typically made of 40% translation/rotation, 40% jump move, 20% swap, the total run length being ~100 million steps. The outcome of the simulation was the mole fraction of each

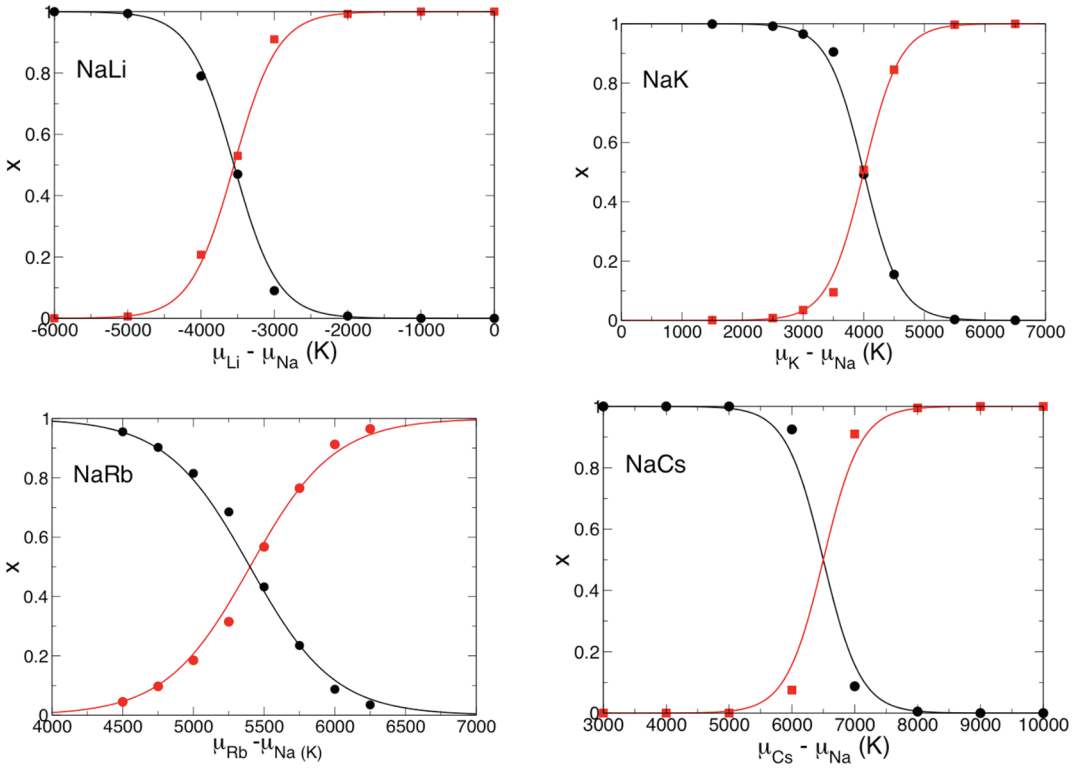

Figure 3. Evolution of the cation mole fraction in bulk water as a function of the chemical potential difference for mixture of NaCl with LiCl (top left), KCl (top right), RbCl (bottom left), and CsCl (bottom right) at 0.1 total molarity and 298 K. The fractions of Na^+ cation are shown as black circles and other cation mole fraction as red squares. Lines correspond to a fit using eq 6 (see the text).

cation within the zeolite at equilibrium. We did not observe any hysteresis with the simulated exchange. The cation exchange isotherms are computed at full equilibrium, and we observed no influence of the starting configuration.

The results of the MC simulations are shown in Figure 1 (lower panel) together with the experimental data of Sherry[17] (upper panel). The agreement between experiments and simulations is, at least qualitatively, remarkable, given that no force field parameter readjustment was made in this work. The simulations are able to capture the main features of the four isotherms, namely, a strong selectivity for the outgoing cation in the case of Na^+/Li^+, a reversal of selectivity for Na^+/K^+, and an incomplete exchange for Na^+/Rb^+ and Na^+/Cs^+. There are of course some quantitative disagreements, and these results should not be oversold. Given the uncertainty of the simulation data (±0.05 in mole fractions), the selectivity reversal in Na^+/K^+ could be considered as doubtful, for instance. Nevertheless, we will now show that a closer examination of the type of cation sites involved at different stage of the process can bring new and useful insights into the underlying mechanism of cation exchange in zeolites.

Let us start with the Na^+/Li^+ exchange (Figure 1, black line), for which the separation factor is lower than 1, whatever the composition of the aqueous solution. The changes in cation configuration within the zeolite for each cationic site, as observed in the simulations, are shown in Figure 4.

The starting equilibrium cation configuration in hydrated $Na_{52}Y$ is such that four cations occupy site I, 16 occupy site I′, and 32 occupy site II. We note such a configuration in the following way: {I(4); I′(16); II(32)}. It should be reminded here that this configuration is different from that of a dehydrated sample: {I(12); I′(8); II(32)}. A cation migration from I to I′ sites is observed upon water adsorption in NaY.[33]

At a lithium mole fraction in the solution of $x_{sol}(Li^+) \sim 0.6$, sodium cations in site I′ begin the exchange with lithum cations in the same site. From $x_{sol}(Li^+) \sim 0.8$ sodium cations in site I are now exchanged by lithium cations that will occupy site I′ as well. In the fully exchanged LiY, no cation is found in site I anymore. The exchange process from $Na_{52}Y$ to $Li_{52}Y$ corresponds to a net migration of four cations from site I to site I′. In the very final stage of the exchange process, sodium cations in site II are exchanged by the same number of lithium cations occupying the same site. The final $Li_{52}Y$ configuration is thus {I(0); I′(20); II(32)}.

This exchange process can be understood in terms of the energetics of the cation−framework interactions. A computation of the interaction potential energies shows that site I is more favorable to Na^+ than to Li^+. This is because of the smaller size of the lithium cation that interacts less efficiently with all the neighboring oxygen atoms in the hexagonal prism. The opposite is true for site I′, which is more favorable to Li^+ because it can get closer to the six ring window of the sodalite cage. Finally, the cation−framework interaction in site II is similar for Na^+ and Li^+, and this explains why the exchange of site II cations takes place at the end of the process.

Although the computed Li^+ exchange isotherm does not perfectly reproduce the experimental one, there are reasons to believe that the simulations capture the essential features of the cation exchange process. No lithium ions have been experimentally detected in site I (in NaLiX as well as in NaLiY).[13] It is also apparent from the literature that a complete lithium exchange is difficult to achieve. As pointed out by Frising and Leflaive[13] in their review paper, in samples where lithium exchange is not complete, lithium ions preferentially occupy sites II and I′. We thus believe that the

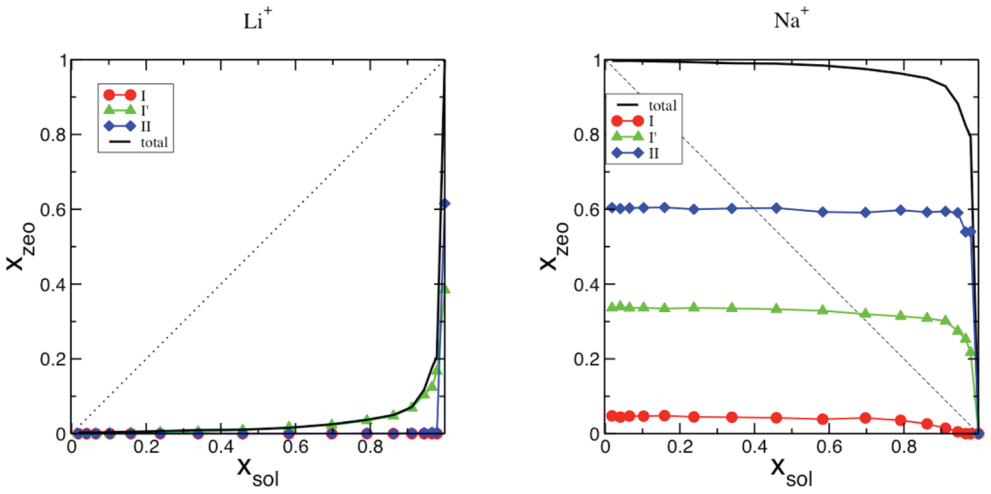

Figure 4. Ion exchange isotherm (black line) for LiNaY zeolite and fraction of the extraframework cations localized in sites I (circles), I′ (triangles), and II (diamonds) for Li^+ (left) and Na^+ (right) cations.

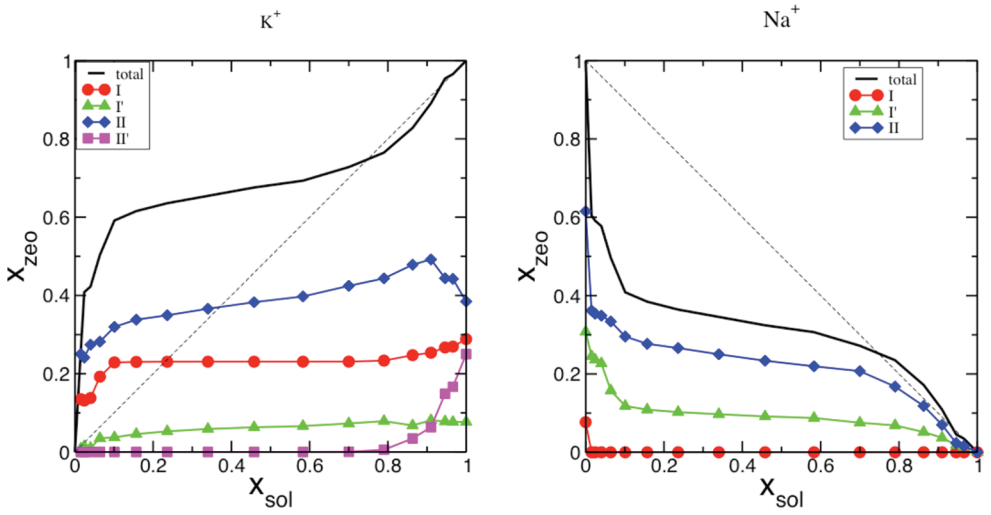

Figure 5. Ion exchange isotherm (black line) for KNaY zeolite and fraction of the extraframework cations localized in sites I (circles), I′ (triangles), and II (diamonds) for K^+ (left) and Na^+ (right) cations.

quantitative disagreements between simulations and experiments can be accounted for, in this case as well as in the other three exchange isotherms, by the drastic simplifications of the models and force fields.

We now address a very crucial thermodynamic point. As pointed out above, the Na^+/Li^+ exchange process is overall energetically favorable, from the point of view of the cation−framework interactions. However, the exchange isotherm is characterized by an exchange selectivity in favor of Na^+ (a separation factor lower than 1)! This issue has been addressed recently in the case of ion exchange in clay minerals. Teppen and Miller[34] have pointed out that the complete energetics of the ion exchange must include the hydration energies of the ions in the aqueous solution, and not only the specific ion−surface interactions, as it was most often considered in the past. This was confirmed by Rotenberg and co-workers,[35] who showed, through a combination of microcalorimetry and molecular simulations, that replacing Na^+ by Cs^+ in interlayer of montmorillonite clays is endothermic and that the overall exchange is exothermic because it is dominated by the exothermic replacement of Cs^+ by Na^+ in the aqueous solution. The isovalent cation exchange in clays is thus dominated by the hydration energy of the cations, the smaller cation being the best hydrated.

Following this line of reasoning, we infer that the replacement of Na^+ by Li^+ in NaY is also dominated by the difference in hydration energy of the ions. Everything occurs as if the aqueous solution "selects" Li^+ over Na^+, because it is more strongly hydrated. The separation (or selectivity) factor α_{Na+}^{Li+} of the zeolite is thus lower than 1, even though the ion−zeolite interactions are in favor of Li^+.

The same concept can be extended to the other cation exchanges studied here. K^+, Rb^+, and Cs^+ are larger cations than Na^+, and thus *less* hydrated in the aqueous solution. The difference in hydration energies then contributes to a separation factor α_{Na+}^{B+} greater than 1 (with B = K^+, Rb^+, or Cs^+). This is indeed what we observe in these three exchange isotherms (Figure 1), in the first half of the exchange process (up to $x_{sol} \sim 0.5$). What we will see further on is that the ion−zeolite interactions are less and

dx.doi.org/10.1021/jp209067n |J. Phys. Chem. B 2011, 115, 15059–15066

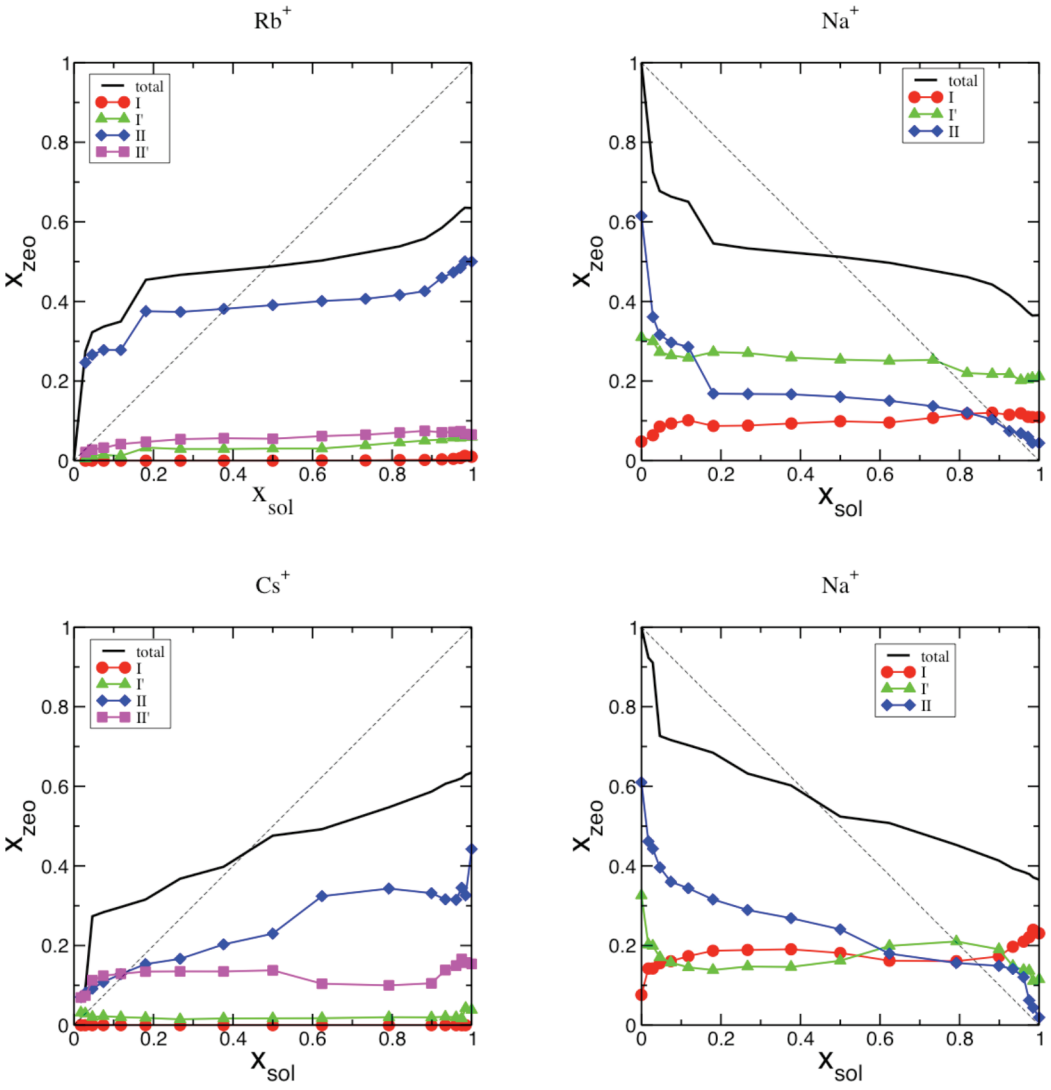

Figure 6. Ion exchange isotherm (black line) for RbNaY (upper panel) and CsNaY (lower panel) zeolite and fraction of the extraframework cations localized in sites I (circles), I′ (triangles), and II (diamonds) for Rb^+/Cs^+ (left) and Na^+ (right) cations.

less in favor of the ingoing cation as the exchange proceeds. In the final part of the exchange process, the ion−zeolite (together with the cation−cation) interactions may become dominant and can lead to a reversal of selectivity. In summary, the hydration energy in the aqueous solution is believed to be the driving force for the cation exchange in zeolite, at least in the range of low mole fraction of the ingoing cation x_{sol}.

Let us now turn to the Na^+/K^+ exchange isotherm represented by the red line in Figure 1. The changes in the cation content are shown in Figure 5. In the first part of the exchange, up to $x_{sol} \sim 0.1$, about half of the cations in sites II are exchanged very rapidly. This is due to the fact that the interaction energies for K^+ and Na^+ are similar, as long as the site II occupancy is not too high. Above a half-occupancy, cation crowding begins to take place in the supercage, because of the larger size of K^+. This first part is also characterized by a net migration of cations from site I′ to site I which is more favorable for K^+ than for Na^+. At this stage, roughly 65% of the Na^+ cations have been replaced. The ion−framework energy balance was in favor of K^+, and this goes in the same direction as the hydration energies in the aqueous solution (see above). The exchange isotherm thus displays a strong selectivity in favor of the ingoing cation K^+. From $x_{sol} = 0.1$ to 0.8, a clear change of slope of the isotherm is observed, and this is correlated with a much lower rate of cation exchange, as seen in Figure 5. The number of K^+ cations in site I has almost reached saturation (14 cations out of 16 theoretically possible). Cations in site II are replaced at a slower pace because of the supercage crowding mentioned above. In this part of the process, the replacement of Na^+ by K^+ becomes more and more difficult because of the larger size of K^+, which means that repulsion between potassium ions begins to take place. In the last part of the process ($x_{sol} > 0.8$) cation crowding becomes critical and the number of cations in site II cannot grow above 20 (while the site II occupancy in NaY is 32). The 12 last K^+ cations can only find a place within the sodalite cages in sites II′ (see Figure 5, left panel), which is an energetically unfavorable site. The final cation configuration is {I(15); I′(5); II(20); II′(12)}. This is clearly correlated with the observed reversal of selectivity. We conclude from this analysis that, while the cation hydration energy is dominant in the first stage of the exchange process (for low x_{sol}), the cation−framework and cation−cation interactions may become dominant in its final part. Whenever the cation−framework and cation−cation interactions

dx.doi.org/10.1021/jp209067n |J. Phys. Chem. B 2011, 115, 15059–15066

become unfavorable for the ingoing cation, a reversal of selectivity may take place.

The last two exchange isotherms (Rb^+, green line and Cs^+ blue line) display a selectivity in favor of the ingoing cation in the first part of the process ($x_{sol} < 0.5$) for the same reasons as in the case of K^+. Above $x_{sol} = 0.5$, a reversal of selectivity takes place and the isotherm ends up with an incomplete exchange. In both cases we find that ~62% of the Na^+ cations are exchanged at the end of the process. This compares quite well with the 68% observed experimentally.[17]

The changes in cation content, as observed in the simulations, are shown in Figure 6, for Rb^+ (upper panel) and Cs^+ (lower panel). The observed trends are similar in both cases. About two-thirds of the cations in sites II are exchanged in a first stage, followed by a plateau and a final drop close to the end of the process, where only two sodium cations are left in site II. Almost all Na^+ cations in site II are then replaced during this incomplete exchange. The situation is quite different for cations in site I′, for which only ~30% of the Na^+ are replaced by Rb^+ or Cs^+. Finally, the most remarkable feature is that the number of sodium cations in site I *increases* from the initial NaY sample to the final $Na_{19}Rb_{33}Y$ or $Na_{20}Cs_{32}Y$ systems. This is more visible in the cesium case, in which the cation content in site I increases from 4 to 12 during the exchange process. Note, in Figure 6 (lower panel, right sketch), the important increase in the number sodium cations in site I at the very end of the exchange process. An *increase* in the number of cations in an exchange process during which the concentration of this very cation *decreases* is quite an unexpected feature. There is no violation of any thermodynamic rule here, since the total number of sodium cations always decreases throughout the process. See for instance the end part of the process (lower panel, right sketch) in which the increase in site I cations is more than compensated by the decrease in sites I′ and II.

The incomplete exchange feature has to do with the particular case of cationic site I in faujasite. This site is located in the middle of the hexagonal prism, connecting two sodalite cages through their six-ring windows. The size of one of these prisms (there are 16 of these cages per unit cell) is such that it can host no more than one cation and no water molecule. From our molecular simulation model, we find that the ion−framework interaction energy is favorable for any of the four cations studied here. This is mostly due to the stabilizing van de Waals and polarization interactions between the cation in site I and the neighboring 12 oxygen atoms of the double six-ring. The size of the univalent cation determines the intensity of its interaction with the framework. When the cation is too small, the interaction is not optimal. As already seen above, the interaction is stronger for sodium than for lithium and also stronger for potassium than for sodium ($Li^+ < Na^+ < K^+$). Above an optimal size, corresponding in our case to potassium, the interaction decreases again because of the repulsive term of the force field that comes into play. Then we have $K^+ > Rb^+ > Cs^+$. Note that this has nothing to do with the fact that a given cation can or cannot penetrate within the hexagonal prism. The above reasoning only relies on the interaction of a given cation that we locate in site I, with the zeolite framework.

What we observe during the simulation runs of NaCsY is that the difference in interaction energies between sodium and cesium cations in site I is such that the cesium ions always find a preference for any other sites, including site II′. At the end of the process ($x_{sol} \rightarrow 1$), the replacement of sodium cations can only take place if some sodium ions migrate to site I. This is a very unusual phenomenon. At the very end of the process, the configuration of the system is {I($12Na^+$); I′($6Na^+$,$2Cs^+$); II-($2Na^+$,$22Cs^+$); II′($8Cs^+$)}. This corresponds to the final state of the system that can be reached using aqueous solution. It must be stressed here that this final state cannot be linked to an inability of the cesium cations to cross the six-ring window in order to penetrate into the hexagonal prism. This "ion sieving" argument was put forward to explain the incomplete exchange feature.[1,2,17] However, in the Monte Carlo simulation, the cation species are displaced randomly. In the swap move introduced above in the Simulation Model and Methods section, a trial move consisting of replacing a sodium cation in site I by a cesium cation was encountered very often. At the end of the MC run, however, not a single cesium cation was found in site I, because of the large difference in ion−framework interaction energy between these two species.

In order to investigate the possibility of obtaining a fully exchanged cesium Y faujasite, we performed an (N,V,T) Monte Carlo simulation in which we fixed the number of cesium cations to 52. This MC simulation ended up with the following stable configuration of $Cs_{52}Y$: {I(12); I′(8); II(24); II′(8)}. Within the model and force field used in these simulations, it appears that a stable fully exchanged CsY is thermodynamically possible. The same simulation was performed in the case of $Rb_{52}Y$, for which we found a very similar stable configuration, {I(14); I′(8); II(22); II′(8)}. It should be mentioned here that the group of Seff has been able to synthesize fully exchanged samples of RbX or CsX obtained by a different means than the conventional aqueous solution exchange, namely, a redox reaction of NaX with rubidium or cesium vapor at 400−450 °C.[36−38] Moreover, 100% exchange samples of CsY have been obtained by using a solid-state ion-exchange method involving the direct reaction of zeolite NH4-Y with CsOH.[39]

We conclude from this analysis of the simulation results that the incomplete exchange corresponds to the stable state of the NaCsY (or NaRbY) system for the highest chemical potential difference accessible in aqueous solution. A stable fully exchanged CsY or RbY state is physically possible but does not seem to be directly reachable by a simple exposure of the bicationic NaCsY (NaRbY) faujasite to an aqueous solution containing Cs^+ (or Rb^+) ions only. This is consistent with the findings of Norby et al.[15] and Koller et al.,[16] who observed by XRD and NMR that a dehydration of the incompletely exchanged NaCsY was accompanied by a migration of sodium ions from site I to the sodalite cages and the supercages, making it possible to further exchange these ions with cesium cations. They also observed a subsequent migration of cesium ions into the smallest cages, including the hexagonal prism,[16] thus demonstrating that a cesium cation could well diffuse through a six-ring window. Repeating calcination (dehydration)−rehydration−exchange cycles four times leads to an exchange level of 83%[15] and 90%.[16] The difference in behavior of cesium cations in the hydrated and dehydrated samples might be attributed to the fact that whenever water is present within the zeolite pore, it is energetically preferable for Cs^+ to be hydrated, whatever the cationic site, instead of sitting on site I. In the absence of water, site I becomes energetically competitive with other sites, especially in the end of the exchange process, where cation crowding becomes important.

CONCLUSION

We have adapted a grand ensemble Monte Carlo simulation method to directly compute, for the first time to our knowledge, univalent cation exchange isotherms in zeolites. The computed

isotherms for the exchange of sodium in NaY faujasite by lithium, potassium, rubidium, and cesium ions, respectively, are in good agreement with the experimental ones. They display the three main types of behavior observed in zeolites, namely, a monotonous evolution of selectivity throughout the exchange process (Li^+), a selectivity reversal (K^+), and an incomplete exchange (Rb^+ and Cs^+). An analysis of the simulation results enabled us to shed some new light on the cation exchange process. The initial stage of the cation exchange is shown to be dominated by the hydration energy of the cations in the external aqueous solution. The final part of the process is often dominated by the cation−framework and cation−cation interactions. A crossover between these two regimes explains the frequently observed reversal of selectivity phenomenon. The incomplete exchange observed in the case of Rb^+ and Cs^+ is correlated with the lack of exchange of cations located in sites I and I′. The difference in interaction energies between sodium and rubidium or cesium cations in site I is such that these large ions always find a preference for any other sites, including site II′. At the end of the process ($x_{sol} \rightarrow 1$), the replacement of sodium cations can only take place if some sodium ions migrate to site I. This leads to an unexpected increase in sodium ion content in site I. At the very end of the process, the system is blocked in a configuration {I($12Na^+$); I′($6Na^+$,$2Cs^+$); II($2Na^+$,$22Cs^+$); II′($8Cs^+$)}. This state is shown not to be linked to an inability of the cesium cations to cross the six-ring window in order to penetrate into the smallest cages. It corresponds to the maximum exchange ratio accessible using aqueous solution.

Direct Monte Carlo simulations of exchange isotherms have been shown to be able to provide some new answers to rather old problems. Work is in progress to extend this study to more complex systems, such as non-univalent exchanges, and also to compute thermodynamic constants in order to improve the simulation force field through a comparison with experiments.

AUTHOR INFORMATION

Corresponding Author

*E-mail: alain.fuchs@cnrs-dir.fr.

ACKNOWLEDGMENT

M.J. is grateful to IFP Énergies Nouvelles (IFPEN) and Association Nationale de la Recherche Technologique (ANRT, France) for her Ph.D. grant. Dr Carlos Nieto-Draghi is gratefully acknowledged for fruitful discussions.

REFERENCES

(1) Sherry, H. S. in *Handbook of Zeolite Science and Technology*; Auerbach, S. M., Carrado, K. A., Dutta, P. K., Eds.; Dekker: New York, 2003; Chapter 21.
(2) Bajpai, D.; Tyagi, V. K. *J. Oleo Sci.* **2007**, *56*, 327–340.
(3) Gu, B. X.; Wang, L. M.; Ewing, R. C. *J. Nucl. Mater.* **2000**, *278*, 64–72.
(4) Brumfiel, G.; Cyranoski, D. *Nature* **2011**, *474*, 135–136.
(5) Mortier, W. J. *Compilation of Extra-Framework Sites in Zeolites*; Butterworths: Guilford, 1982.
(6) Baerlocher, C.; McCusker, L. B.; Olson, D. H. *Atlas of Zeolite Framework Types*; Elsevier: New York, 2007.
(7) Vitale, G; Mellot, C. F.; Bull, L. M.; Cheetham, A. K. *J. Phys. Chem. B* **1997**, *101*, 4559.
(8) Sanders, M. J.; Catlow, C. R. A.; Smith, J. V. *J. Phys. Chem.* **1984**, *88*, 2796.
(9) Smolders, E.; Van Dun, J. J.; Mortier, W. J. *J. Phys. Chem.* **1991**, *95*, 9908.
(10) Jaramillo, E.; Auerbach, S. M. *J. Phys. Chem. B* **1999**, *103*, 9589.
(11) Buttefey, S.; Boutin, A.; Mellot-Draznieck, C. F.; Fuchs, A. H. *J. Phys. Chem. B* **2001**, *105*, 9569.
(12) Beauvais, C.; Guerrault, X.; Coudert, F.-X.; Boutin, A.; Fuchs, A. H. *J. Phys. Chem. B* **2004**, *108*, 393.
(13) Frising, T.; Leflaive, P. *Microporous Mesoporous Mater.* **2008**, *114*, 27–63.
(14) Breck, D. *Zeolite Molecular Sieves: Structure, Chemistry and Use*; Krieger Pub. Co.: Malabar, FL, 1984; Chapter 7.
(15) Norby, P.; Poshni, F. I.; Gualtieri, A. F.; Hanson, J. C.; Grey, C. P. *J. Phys. Chem. B* **1998**, *102*, 839–856.
(16) Koller, H.; Burger, B.; Schneider, A. M.; Engelhardt, G.; Weitkamp, J. *Microporous Mater.* **1995**, *5*, 219–232.
(17) Sherry, H. S. *J. Phys. Chem.* **1966**, *70*, 1158–1168.
(18) Fitch, A. N.; Jobic, H.; Renouprez, A. *J. Phys. Chem.* **1986**, *90*, 1311–1318.
(19) Lachet, V.; Boutin, A.; Tavitian, B.; Fuchs, A. H. *Langmuir* **1999**, *15*, 8678–8685.
(20) Lachet, V.; Buttefey, S.; Boutin, A.; Fuchs, A. H. *Phys. Chem. Chem. Phys.* **2001**, *3*, 80–86.
(21) Di Lella, A.; Desbiens, N.; Boutin, A.; Demachy, I.; Ungerer, P.; Bellat, J.-P.; Fuchs, A. H. *Phys. Chem. Chem. Phys.* **2006**, *8*, 5396–5406.
(22) Jorgensen, W. L.; Chandrasekhar, J.; Madura, J. D.; Impey, R. W.; Klein, M. L. *J. Chem. Phys.* **1983**, *79*, 926–935.
(23) Jaramillo, E.; Grey, C. P.; Auerbach, S. M. *J. Phys. Chem. B* **2001**, *105*, 12319–12329.
(24) Di Lella, A. 2007, Ph.D. Thesis, Université de Paris-Sud, Orsay, France.
(25) Dang, L. X. *J. Am. Chem. Soc.* **1995**, *117*, 6954–6960.
(26) Uytterhoeven, L.; Dompas, D.; Mortier, W. J. *J. Chem. Soc. Faraday Trans.* **1992**, *88*, 2753–2760.
(27) Nicholson, D.; Parsonage, N. G. *Computer Simulation and the Statistical Mechanics of Adsorption*; Academic Press: New York, 1982
(28) Lachet, V.; Boutin, A.; Tavitian, B.; Fuchs, A. H. *Faraday Discuss.* **1997**, 307–323.
(29) Sindzingre, P.; Ciccotti, G.; Massobrio, C.; Frenkel, D. *Chem. Phys. Lett.* **1987**, *136*, 35–41.
(30) Sindzingre, P.; Massobrio, C.; Ciccotti, G.; Frenkel, D. *Chem. Phys.* **1989**, *129*, 213–224.
(31) Widom, B. *J. Chem. Phys.* **1963**, *39*, 2808.
(32) Yan, Q.; de Pablo, J. J. *J. Chem. Phys.* **1999**, *111*, 9509.
(33) Beauvais, C.; Boutin, A.; Fuchs, A. H. *Chem. Phys. Chem.* **2004**, *5*, 1791.
(34) Teppen, B. J.; Miller, D. M. *Soil Sci. Soc. Am. J.* **2005**, *70*, 31–40.
(35) Rotenberg, B.; Morel, J.-P.; Marry, V.; Turq, P.; Morel-Desrosiers, N. *Geochim. Cosmochim. Acta* **2009**, *73*, 4034–4044.
(36) Lee, S. H.; Kim, K.; Seff, K. *J. Phys. Chem. B* **2000**, *104*, 11162–11167.
(37) Sun, T.; Seff, K.; Heo, N. H.; Petranovskii, V. P. *Science* **1993**, *259*, 495.
(38) Sun, T.; Seff, K.; Heo, N. H.; Petranovskii, V. P. *J. Phys. Chem.* **1994**, *98*, 5768–5772.
(39) Weitkamp, J.; Ernst, S.; Hunger, M.; Roser, T.; Huber, S.; Schubert, U. A.; Thomasson, P.; Knozinger, H., Stud. *Surf. Sci. Catal* **1996**, *101*, 731.